Journal of
Pharmacology & Clinical Toxicology

SciMedCentral

Special Issue on
Pharmacokinetics and Pharmacodynamics

Review Article

The clinical role of nuclear imaging in immunotherapeutic drug development

BerlindaJ. de Wit – van der Veen*, Marcel P.M. Stokkel

Department of Nuclear Medicine, NKI-AVL, Netherlands

Abstract

Advances in the oncological sciences have led to the development of agents that are designed to affect specific molecular pathways. However, many of these immunotherapeutic agents do not successfully pass phase 2 trials due to concerns with efficacy, toxicity or side effects. The generalized endpoints that traditionally have been used in these trials, such as maximum tolerated dose and overall response, may be less optimal for immunotherapeutic agents. The addition of in vivo nuclear imaging in these early trials can aid in patient stratification, evaluation of drug bio distribution, pharmacodynamic effects and tumor heterogeneity. This review discusses the advantages of nuclear imaging, and outlines the first application of these imaging biomarkers in clinical trials.

***Corresponding author**

Berlinda J. de Wit – van der Veen, Department of Nuclear Medicine, NKI-AVL, Plesmanlaan 121, 1066 CX Amsterdam, the Netherlands; Tel: 31-20 512 2287; Fax: 31-20 512 2290; Email: l.vd.veen@nki.nl

Submitted: 04 May 2015

Accepted: 17 August 2015

Published: 20 August 2015

Keywords

- Positron emission tomography
- Biodistribution
- Immunotherapeutic agents
- Imaging biomarker

ABBREVIATIONS

SPECT: Single Photon Emission Computer Tomography, PET: Positron Emission Tomography, CT: Computer Tomography, MRI: Magnetic Resonance Imaging, HER2: Human Epidermal Growth Factor 2, VEGF: Vascular Endothelial Growth Factor, EGFR: Epidermal Growth Factor Receptor, GCPII or PSMA: Glutamate Carboxypeptidase II, CAIX: Carbonic Anhydrase 9, RIT: Radioimmunotherapy

INTRODUCTION

Anticancer drugs have traditionally been discovered either by chance or by widespread screening programs. However, the progress in molecular and genetic oncological sciences has led to the identification of new drug targets. This resulted in a paradigm shift towards the development of anticancer agents that are specifically designed to affect one or multiple molecular pathways. Unlike conventional cytotoxic drugs, most of which disrupt processes in the nucleus, these compounds can affect the tumor microenvironment, transmembrane or intracellular processes. The triggered effects are often aimed at inhibiting tumor growth and limiting metastatic progression (cytostatic), rather than directly kill tumor cells (cytotoxic) [1].

Among the first immunotherapeutic agents to receive FDA approval were compounds like Rituximab (Rituxan, Biogen Idec, 1997), Trastuzumab (Herceptin, Genentech, 1998), and Cetuximab (Erbitux, Bristol-Myers Squibb, 2003). Still, many target-based therapies do not successfully pass phase 2 trials due to concerns with efficacy, toxicity or side effects. This has raised the question whether traditional pharmacological studies (e.g., preclinical, phase 1, phase 2, etc.) are optimal for these drugs [2,3]. Traditionally, phase 1 trials seek to determine the optimal dose scheme and general efficacy of a new drug in humans. The main endpoints consist of aspects like maximum tolerated dose, biological dose range and tumor response. However, these generalized endpoints do not reflect the true complexity and individualization of targeted therapeutic agents.

Identification of key molecular oncogenic pathways or drivers in a set population is the foundation for targeted-drug development. Consequently, molecular stratification of patients is vital for successful clinical implementation of immunotherapeutic agents. Biomarkers that provide specifics on the drug-target are preferably identified during compound design and preclinical evaluation. In early clinical trials, imaging biomarkers are increasingly used as they can attribute in patient selection, tumor characterization and early response assessment [4,5].

Imaging in drug development

Anatomical imaging modalities, such as computer tomography (CT) and magnetic resonance imaging (MRI) are generally used to localize lesions and evaluate tumor shrinkage. Radiological assessment of therapy response or disease progression is performed according to the highly standardized 'Response Evaluation Criteria in Solid Tumors'- or RECIST-criteria. Additionally, image-guided biopsies are performed to evaluate the local pharmacodynamic effects in specific target lesions. These conventional strategies to identify tumor load and response have however some important drawbacks; 1) they only provide a generalized estimate of response, 2) they do not take tumor heterogeneity into account, and, 3) they do not provide characteristics on the drug-target within the tumor lesions.

In the era of targeted therapies, nuclear molecular imaging has gained popularity as a method to characterize tumors *in vivo*. In itself this approach is not new, and has been used for decades in cell cultures and tissue slices. *In vivo* nuclear imaging relies on the administration of a radioactive isotope coupled to a biological compound (e.g., radiopharmaceutical), and on the detection of radiation emitted by the isotope. The resulting images represent specific biological processes, rather than detailed anatomical structures. The radiopharmaceutical concentration that can be detected with nuclear imaging modalities is in the range of picomolar, whereas for contrast-based anatomical imaging modalities such as CT and MRI, these concentrations are in the order of millimolar. This ensures that nuclear imaging can be performed using micro dosages of the biological active compound to aid in early clinical studies [6,7]. This strength explains the wide spread use of nuclear imaging in therapeutic drug development to visualize biodistribution, target occupancy, pharmacodynamic effects, tumor heterogeneity, or just to localize tumor targets before or during treatment [8-10]. This approach holds great benefit as it increases the power of trials, optimizes treatment schemes and provides background on pharmacodynamic measures.

Translational nuclear imaging techniques

The fore most advantage of radiochemical tracing is the ability to quantify biodistribution and metabolism *in vivo* or *ex vivo* depending on the techniques used. The most widely used imaging techniques in translational drug development include autoradiography, scintigraphy, and positron emission tomography (PET), which will be briefly introduced in the next sections [11].

Autoradiography

Ever since the mid-1900s quantitative whole-body autoradiography has been a valuable tool in preclinical pharmaceutical research. Although, newer techniques like mass spectrometry are available to quantify specific compounds without the need for radioactive labeling, autoradiography is still used today due its highly reproducible nature [12,13]. Typically, the first step of *ex vivo* autoradiography involves the design and production of a drug labelled with long-lived beta-emitting isotopes like Hydrogen (^{3}H), Carbon (^{14}C) or Phosphorus (^{32}P). After administration of the radiolabelled drug, the specimen is quickly cryosectioned (typically 20-50 micrometer). The sections are placed between detector layers, such as X-ray film or phosphorous detector plates, and are left for period of time (typically hours-days). When quantitative evaluation is desired, radioactive calibration standards are placed alongside the specimens. The resulting digital images provide information on tissue concentrations and biodistribution. Micro-autoradiography can be applied to localize radiolabelled compounds at a cellular level when there is a specific organ or tissue of special interest. After image development, the resulting images can be combined with immunohistochemical staining to assess radioactivity accumulation in relation to specific molecular targets. The achieved resolution of autoradiography is dependent on the detector material, isotope (e.g., high energy beta-emitters provide blurred images) and distance between detector plates and specimen, but can range from 10-100 μm [12,14,15].

Scintigraphy

Scintigraphic imaging relies on the detection of single gamma-rays emitted by isotopes using one or multiple large detectors, known as a gamma camera. This imaging technique has been around for almost 60 years, and is routinely used in the clinical practice for a broad range of indications (e.g., cardiology, neurology, orthopedics, oncology, etc.). A gamma camera produces two-dimensional images of a relatively large body area, also known as planar acquisitions. Single photon emission computer tomography (SPECT) is similar to conventional planar imaging, but uses a gamma camera that rotates around the patient and acquires images from different angles. Three-dimensional representations of the isotope distribution are produced after a set of mathematical procedures known as image reconstruction [16]. After proper calibration of the camera, SPECT has the ability to both visualize and quantify radioactivity distributions in structures larger then roughly 1.5cm in size. Depending on the radiopharmaceutical and clinical indication, specific protocols regarding subject preparation, administration, image acquisition and quantification are applied.

Positron emission tomography

Positron emission tomography like SPECT, positron emission tomography (PET) is also a three-dimensional nuclear imaging modality, but has roughly a 10-fold higher sensitivity, increased accuracy, and hence, superior quantitative analysis of images. Unlike the gamma camera, which has multiple rotating detectors, the PET scanner consists of a continues ring with numerous stationary detector elements. When a PET-isotope decays, a positron is emitted that, after collision with an electron, is converted into two photons that are emitted under a 180 degree angle (e.g., the process is called annihilation). All these photon-pairs are detected by the opposing detector elements in the PET-ring. After image reconstruction, three-dimensional

representations of the isotope distribution are produced in which structures of ~5mm in size can be evaluated. The principal isotope used for traditional PET imaging in oncology is Fluor-18 (^{18}F) labeled to the glucose-analog fluorodeoxyglucose [17]. Both PET and SPECT are regularly combined with low-dose CT for anatomical localization of specific findings. Also, MRI scanners are increasingly incorporated into PET systems [18].

The differences between SPECT and PET regarding image quality and sensitivity are far less profound for small animal imaging. Because SPECT-isotopes emit low-energy radiation compared to PET-isotopes, a relatively larger portion of the radiation is absorbed within tissue. Small animals have less volume and mass compared to humans, so radiation will better penetrate through the subject, and hence, relatively more radiation will be detected by the SPECT scanner. Additionally, great technological improvements have been made in the last decade. The newest generation commercially available animal SPECT systems are able to provide ultra-high-resolution images for identification of structures below 0.5mm in size [19]. *In vivo* quantification of whole body biodistribution over time and multi-isotope imaging are other important developments. These advances enhanced the role of preclinical nuclear imaging in drug development, and accordingly, its use in clinical trials.

Clinical radiopharmaceuticals

For *in vivo* imaging specific biological and physics-related requirements have to be met; 1) appropriate decay characteristics, 2) the labeling should not influence pharmacokinetics and biodistribution of the drug, and, 3) possibility of easy and stable labeling. The choice of an isotope depends not only on the chemistry of the drug, but also on its biological half-life. If the drug is for instance a small molecules or antibody fragments and has fast kinetics, isotopes with a short half-life (i.e., minutes to hours) should be used. Whereas for intact antibodies that have a half-life of several days, isotopes with a matching physical half-life are used. Depending on the radioisotope and molecular structure of the drug, different radiolabeling strategies can be applied. Still, the biological behavior of the radiopharmaceutical with respect to the biodistribution and pharmacokinetics should be similar to the unlabeled drug. Additionally, targeting of the drug should be good, and off-target binding of the radiolabelled drug should be minimal, to reduce the radiation dose to the patient. The final consideration for isotope selection is related to decay characteristics and the type of imaging modality that will be used. Isotopes that emit gamma rays are used for scintigraphic imaging, whereas positron emitters are used for PET. Table 1 provides an overview of the most important isotopes used in translational pharmacological research.

Focus on antibody PET in clinical trials

Several antibodies have been radiolabelled in the developmental phase or shortly after clinical introduction to characterize lesions, quantify response or to select suitable patients for immunotherapy. Table 2 provides an extended overview of all the listed clinical trials that have been performed with the key PET isotopes ^{89}Zr, ^{64}Cu and ^{124}I.The following paragraphs will focus on targets that have been used in a clinical setting, including CD20, CD44, human epidermal growth factor 2 (HER2), vascular endothelial growth factor (VEGF), epidermal growth factor receptor (EGFR), glutamate carboxypeptidase II (GCPII, also known as PSMA), and carbonic anhydrase 9 (CAIX) (marked with a star in Table 2).

CD20-targeting (B-cell lymphoma)

Retuximab and ibritumomabtiuxetan belong to the first tumor-targeted therapies approved by the FDA, both as a monotherapy and in combination with other chemotherapies.

Table 1: Important radionuclides used in translation clinical studies.

		Half-life	Main emitter, E_{max} (yield %)
Autoradiography & ADME studies			
Carbon-14	^{14}C	>5700 y	ß-, 0.156 MeV (100)
Hydrogen-3	^{3}H	12.3 y	ß-, 0.019 MeV (100)
Phosphorus-32	^{32}P	14.3 d	ß-, 1.709 MeV (100)
SPECT			
Technetium-99m	^{99m}Tc	6.0 h	Y, 142 keV (90)
Indium-111	^{111}In	2.81 d	Y, 171 keV (90.2) and 245 keV (94.0)
Iodine-131	^{131}I	8.0 d	Y, 364 keV (82)
PET			
Oxygen-15	^{15}O	2 min.	ß+, 1.73 MeV (99,9)
Carbon-11	^{11}C	20 min.	ß+, 0.98 MeV (99,8)
Gallium-68	^{68}Ga	68 min.	ß+, 1.89 MeV (89.1)
Fluor-18	^{18}F	109 min.	ß+, 0.633 MeV (96.7)
Copper-64	^{64}Cu	12.7 h	ß+, 0.653 MeV (17.4)
Zirconium-89	^{89}Zr	78.4 h	ß+, 0.897 MeV (22.7)
Iodine-124	^{124}I	100.3 h	ß+, 1.54 MeV (11.8) and 2.14 MeV (10.9)

Abbreviations: E_{max} Maximal energy, y years, d days, h hours, min. minutes, keV kilo electron Volt, MeV Mega electron Volt

Table 2: Overview of clinical studies with 89Zr-, 64Cu- or 124I-labelled antibodies or fragments [A].

Radiopharmaceutical	Target	Tumor types	# of trials (# completed)
^{89}Zr-Bevacizumab	VEGF *	Multiple Myeloma|Breastcancer|RCC|NET	8 (6)
^{89}Zr-Trastuzumab	HER2 *	Breastcancer|Esophagogastriccancer	8 (1)
^{89}Zr-Cetuximab	EGFR *	Colorectal cancer	3 (2)
^{89}Zr-Panitumumab	EGFR *	NSCLC|Urothelialcancer|Sarcomas	1 (0)
^{89}Zr-huJ591	PSMA *	Prostatecancer|Glioblastoma	2 (0)
^{89}Zr-Df-IAB2M	PSMA *	Prostate cancer	3 (0)
^{89}Zr-Girentuximab	CA-IX *	RCC	1 (0)
^{89}Zr-RO5429083	CD44 *	CD44-expressing solid tumors	1 (1)
^{89}Zr-MSTP2109A	STEAP1	Prostate cancer	1 (0)
^{89}Zr-DS-8895a	EphA2	EphA2-expressing solid tumors	1 (0)
^{89}Zr-MMOT0530A	MLSN	Pancreaticcancer|Ovariancancer	1 (0)
^{89}Zr-GSK2849330	HER3	HER3-expressing solid tumors	1 (0)
^{89}Zr-GC1008	TGF-β	Gliomas	1 (0)
^{64}Cu-Trastuzumab	HER2 *	Breastcancer|Esophagogastriccancer	4 (1)
^{64}Cu-Rituximab	CD20 *	Lymphoma	1 (0)
^{64}Cu-M5A IV	M5A	CEA-expressing solid tumors	1 (0)
^{64}Cu-U3-1287	HER3	HER3-expressing solid tumors	1 (1)
^{64}Cu-Plerixafor	CXCR4	Solid tumors	1 (0)
^{64}Cu-AE105	uPAR	Prostate cancer|Breastcancer|Urothelial cancer	1 (1)
^{124}I-cG250	CAIX *	RCC	6 (4)
^{124}I-hu3F8	GD2	Melanoma|Neuroblastoma|Sarcoma	1 (0)
^{124}I-anti8H9	8H9	Peritonealcancer|Gliomas|Neuroblastoma	2 (0)
^{124}I-huA33	A33	Colorectal cancer	1 (0)
^{124}I-PGN650	PS	Solid tumors	1 (0)

[A] This overview only includes completed and active trials registered at the ClinicalTrails.gov database.
Abbreviations: RCC: Renal Cell Carcinoma; NET: Neuroendocrine Tumors; NSCLC: Non-Small Cell Lung Cancer

Lymphoma's are typically very radiosensitive, so it did not take long before these antibodies were radiolabeled with α- or β-emitting isotopes to provide targeted radiotherapy (also known as radioimmunotherapy) or with γ-emitting isotopes for imaging. At this moment, two FDA-approved radiopharmaceuticals are available for the treatment of lymphoma, Yttrium-90 (^{90}Y) ibritumomabtiuxetan (Zevalin) and ^{131}Itositumomab (Bexxar), both of which are directed against different epitopes of CD20 [20]. Currently, well over 60 completed or ongoing clinical trials with radiolabelled retuximab or ibritumomabtiuxetan are registered. Prior to radioimmunotherapy (RIT), proper patient selection is crucial, thus tumor load, biodistribution and dosimetry are evaluated with either ^{111}In, ^{89}Zr or ^{64}Cu anti-CD20 imaging [21-25] for example coupled ^{89}Zr to ibritumomabtiuxetan to predict the biodistribution of ^{90}Y-ibritumomabtiuxetan and identify the dose limiting organs in seven patients with CD20-positive B-cell lymphoma [26]. Rituxan was given one week before injection of ±70MBq 89Zr-ibritumomab tiuxetan, as is done in standard ^{90}Y-ibritumomab tiuxetan treatments. Most intense accumulation was seen in the liver and spleen, and the whole body effective dose was ±0.87 mSv/MBq. The correlation between the pre-treatment ^{89}Zr-PET and the actual distribution of ^{90}Y was high, suggesting that PET can be used to predict the therapy biodistribution. For the other CD20 tracers similar results were achieved in the (pre-) clinical setting.

CD44-targeting (head/neck carcinoma, solid tumors)

Many types of solid tumors, among which squamous cell carcinoma of the head and neck (HNSCC), express moderate to high levels of CD44. All efforts of radiolabeling CD44-targeting antibodies were initially focused on RIT, however, application was with variable success. Borjesson et al. were the first to use the ^{89}Zr-labeled anti-CD44v6 chimeric monoclonal antibody cU36 in 20 patients to localize and characterize HNSCC lesions [27]. All primary tumors were visualized and 18 of the 25 tumor-containing lymph node levels were correctly identified. A dosimetric evaluation indicated that the highest observed dosage was found in the liver (±1.3 mSv/MBq), followed by the kidneys, thyroid, lungs and spleen [28]. The average radiation dose to the whole body was 0.6 mSv/MBq. A preclinical evaluation of the novel ^{89}Zr-labelled RO5429083, a humanized anti-CD44 that binds to another epitope, shows promising results in mice and monkeys [29]. Recently, a clinical trial with this drug was completed in which the tissue distribution and pharmacokinetics were assessed using PET.

HER2-targeting (breast & gastric carcinoma)

Approximately a decade ago the first preclinical studies emerged using ^{111}In-Trastuzumab SPECT to evaluate HER2-expression in xenograft tumor models. Though, ^{111}In-Trastuzumab was highly stable *in vivo* and the accumulation was related to HER2-expression, translation to humans proved not feasible due to poor imaging characteristics [30]. Dijkers et al. published the first in-human biodistribution study with a clinical grade ^{89}Zr-Trastuzumab (37MBq). The results indicated that unlabeled-Trastuzumab should be co-administered with the ^{89}Zr-Trastuzumab in both Trastuzumab-naïve (50mg) and on-treatment (10mg) patients to limit off-target accumulation. At appropriate antibody dosages, tumor lesions could be visualized 4-5 days after injection [31,32]. Mortimer et al. and Tamura et al. showed that ^{64}Cu-DOTA-Trastuzumab is also able to visualizes HER2-positive tumor load in metastatic breast cancer, despite the much shorter half-life of ^{64}Cu compared to ^{89}Zr [33,34]. The main advantage of ^{64}Cu over ^{89}Zr, is alowered radiation dose for the patients. Still, both tracers showed substantial accumulation in the blood pool (only in the first 1-2 days), liver, kidney, spleen and bladder.

Other groups have used this imaging approach to assess the pharmacodynamics of novel targeted therapies like PU-H71 (i.e., heat shock protein 90 (HSP90) inhibitor) and afatinib (i.e., EGFR and HER2 tyrosine kinase inhibitor) in small animals [35,36]. Also in patients with metastatic HER2-positivebreast cancer, ^{89}Zr-Trastuzumab PET has successfully been used to evaluate pharmacodynamics of the novel HSP90 inhibitor, NVP-AUY922, and the novel anti-HER2 drug, T-DM1 [37,38]. Though small scale and ongoing, both studies suggest that an early response to treatment could be visualized. A substantial heterogeneous response throughout the lesions within and among patients was observed in both studies. The clinical implications of this heterogeneous HER2-related accumulation in proven HER2-positive breast cancer are still under investigation. Additionally, ^{89}Zr-Trastuzumab imaging (37MBq/50mg)was used in specific clinical dilemmas when biopsies cannot be performed or the patient has a complex medical history with HER-positive and HER-negative tumors [39].

VEGF-targeting (solid tumors)

Though various factors are known to contribute to angiogenesis in solid tumors and metastatic lesions, VEGF is among the most prominent. The anti-VEGF mAbBevacizumab (Avastin) was labeled with ^{111}In and ^{123}I for SPECT imaging with limited success. Cai et al. for the first time demonstrated PET imaging of ^{64}Cu-DOTA-VEGF$_{121}$ (i.e., antibody fragment of Bevacizumab) in a glioblastoma mouse model [40]. Whereas, van der Bilt et al. were the first to use ^{89}Zr-labeled Bevacizumab as an imaging biomarker to study the antiangiogenic effect of everolimus in an ovarian xenograft model [41]. Both Van Asselt et al and Oosting et al. used this same approach in humans to evaluate the effect of antiangiogenic treatment with serial ^{89}Zr-labeled Bevacizumab in neuroendocrine (NET) and renal cell carcinoma (RCC) [42-44]. In these studies, a typical antibody distribution was seen in normal organs with highest accumulation in the circulation, kidneys, liver and spleen four days after injection (37MBq/5mg). Like with ^{89}Zr-Trastuzumab, a highly heterogeneous accumulation pattern was visualized within and among patients. In primary breast cancer, Gaykema et al. used ^{89}Zr-Bevacizumab (37MBq/5mg) successfully to localize lesions with a diameter larger then 10mm (96.1% of lesions visualized) [45].

EGFR targeting (Colorectal & head/neck carcinoma)

Though several EGFR-directed therapies have been developed, the approved antibodies cetuximab and panitumumab are the main targets used in imaging studies. In preclinical studies mixed results are achieved with these ^{64}Cu- and ^{89}Zr-labelled antibodies [46-51]. Aerts et al. demonstrated a disparity between radioactivity accumulation in three positive tumor cell lines and the *ex vivo* EGFR expression [52]. The group of Chen et al. also showed this disparity, which was especially profound in HNSCC tumor models [48-50]. A number of factors could explain these conflicting results, like suboptimal antibody concentration or imaging time points and reduced tumor vascularity or vascular permeability. Nevertheless, these early findings probably have restricted the use of EGDR-PET as imaging biomarker in clinical trials. Only recently, Makris et al. reported on the biodistribution and dosimetry of ^{89}Zr-labeled cetuximab in seven patients with colorectal cancer [53]. The ^{89}Zr-Cetuximab administration (37MBq) was preceded by infusion of unlabeled cetuximab (500mg/m^2). The average effective whole-body dose was 0.61mSv/MBq, and highest radioactivity accumulation was observed in the liver, kidneys, spleen and lungs. At this moment there are two ongoing clinical trials in patients with colon carcinoma to include ^{89}Zr cetuximab PET as a method for image guided treatment optimization.

PSMA-targeting (prostate carcinoma)

This target for prostate cancer was already investigated as a possible treatment strategy in androgen resistant metastatic disease in the early 1990's. The first approved imaging antibody, an ^{111}In-labelled anti-PSMA antibody known as *ProstaScint™* (^{111}In capromabpendetide, EUSA Pharma), was introduced for the detection of soft tissue and bone metastasis [54]. However, routine use of *ProstaScint™* was found to be restricted due to suboptimal targeting characteristics resulting in a low sensitivity for detecting metastases, especially in smaller lesions. Other ligands that target the PSMA receptor have been evaluated ever since. Initial attempts focused on intact antibodies that target the extracellular domain and are internalized upon binding [55]. The first results of a pilot study with ^{89}Zr-J591 PET in 11 men with localized PCa showed promising results. First 20mg of unlabeled J591 was infused before injection of 185MBq/2mg ^{89}Zr-J591, and acquisitions were made 5-7 days post injection. A subsequent study to assess the ability of ^{89}Zr-J591 PET to detect lesions and pharmacokinetics of this tracer are still ongoing [56]. Additionally, a number of small molecule inhibitors and antibody fragments, which have considerably faster kinetics but still target the extracellular domain of PSMA, are also used in clinical trials [57,58].

CAIX-targeting (RCC)

Since its discovery in the early 1990's, G250/CAIX was indicated as a promising biomarker in renal cell carcinoma (RCC)

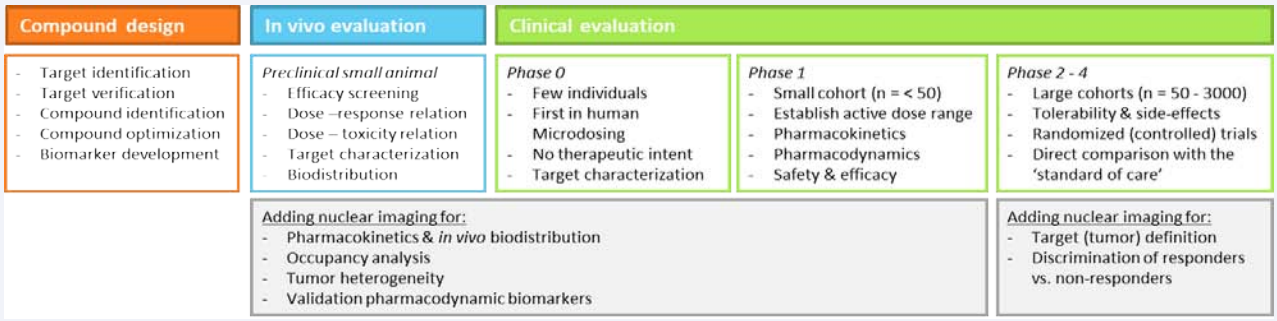

Figure 1 Schematic overview of the traditional pharmacological study design and the role of nuclear imaging within (pre)clinical studies.

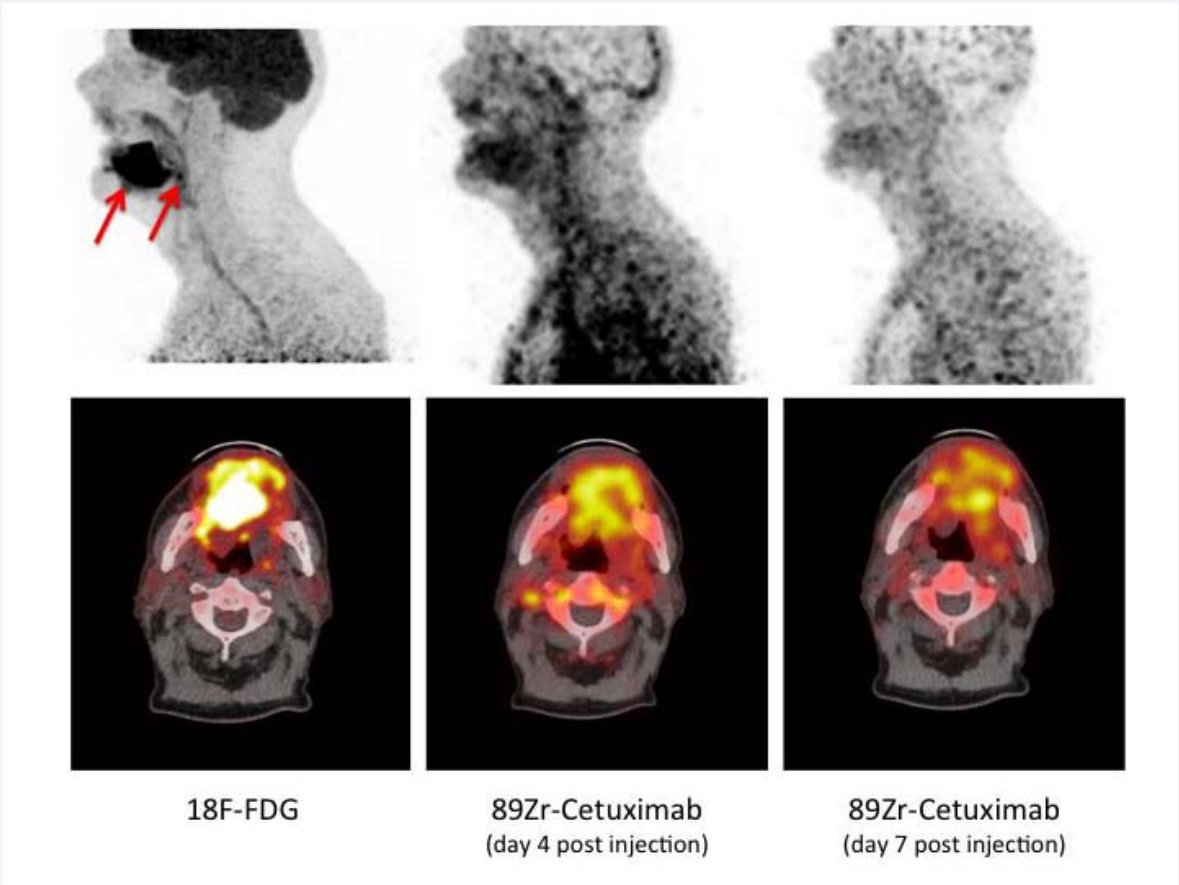

Figure 2 Cetuximab PET-imaging in a patient with HPV-negative HNSCC. As part of a clinical trial ^{89}Zr-Cetuximab (60 MBq) was administered [66]. On the FDG-PET a large primary tumor with high glucose metabolism is visualized in the oral cavity, together with one positive node metastasis (red arrows). On the early ^{89}Zr-PET extensive accumulation is seen both in the circulation and at the site of the primary tumor. On the late ^{89}Zr-PET accumulation is still visible at the site of the tumor, while the activity in the circulation has greatly reduced. At later time-points accumulation in the bone marrow can be visible. Furthermore, there is a marked difference in image quality between the ^{89}Zr and ^{18}F PET.

as it has good targeting characteristics and limited expression in normal tissues [59]. Radiolabeling of G250 (also known as Girentuximab) has been performed by various groups to differentiate between benign versus malignant renal masses, and to study its biodistribution as preliminary work for RIT. The first clinical study in humans with ^{124}I-cG250 by Divgi et al. demonstrated in 26 patients with renal masses that a positive PET scan was highly predictive of clear-cell RCC (sensitivity 94%; specificity 100%) [60]. Radioactivity accumulation as visualized by PET and digital autoradiography was directly related to CAIX expression by immunohistochemistry [61]. Based on these results, a large Phase 3 trials was initiated to validate ^{124}I-cG250 as an imaging biomarker in RCC [62]. A total of 195 patients received a ^{124}I-PET/CT scan 2-6days post-injection (185MBq/13.7mg) and underwent surgery. This study confirmed the initial results of the pilot study, an average sensitivity and specificity of respectively 86.2% and 85.9% were found. It was concluded that ^{124}I-cG250 PET/CT is able to characterize a malignant phenotype, which

could have a major impact on patient management. The first results of preclinical studies with ^{89}Zr-labelled cG250 suggest that this tracer might have better binding and internalization characteristics compared to ^{124}I-cG250 [63]. Accordingly, a clinical trial has been initiated to identify patients suspected of RCC with a less aggressive tumor type using ^{89}Zr-cG250 PET in which watchful waiting can be considered.

Future directions of antibody PET

The great potential of nuclear imaging during the clinical introduction of immunotherapeutic agents has been presented in this overview. The growing use of especially ^{89}Zr-based imaging in clinical multicenter studies has led to a need for harmonization of imaging protocols among the different centers. The use of quantitative imaging biomarkers to describe pharmacokinetics and pharmacodynamics is only valuable if the exchange of those findings among different centers is possible. Recently, the EATRIS (European Infrastructure for Translational Medicine) and the EANM (European Association of Nuclear Medicine) collaborated to facilitate a standardization and cross-calibration program for PET-scanners, as has already been initiated for ^{18}F imaging.

Up to now, most clinical imaging trials with immunotherapeutic agents have been using intact radiolabeled antibodies. Due to the long biological half-life of these compounds imaging is carried out up to 9 days after injection, so ^{124}I and ^{89}Zr are the most suitable isotopes. Though radiolabeling with Iodine is common practice in many labs, looking at imaging characteristics ^{89}Zr has better properties. Several centers are currently involved in the development of new and easier ^{89}Zr-labeling procedures to manufacture stable compounds. Still, both isotopes share common problems, 1) a limited availability due to the dependency of a cyclotron for their production, and, 2) a high radiation burden to the patients due to long residence times of the isotope in the body. As a results, the administered dose is typically between 37 and 100MBq, which in term results in less optimal images and long acquisition times (i.e., >45 minutes for typical whole body acquisition). Despite these extended acquisition times, lesions smaller than 1cm in diameter should not be quantified, and can even are entirely missed on ^{89}Zr and ^{124}I PET. Due to the high radiation dose per injection, imaging with these isotopes can only be performed a limited number of times and in a specific patient population. To put this in perspective, a conventional FDG-PET scan is ±5 mSv, a diagnostic abdominal CT ±8mSv, and an ^{89}Zr-immunoPET ±20-40mSv. Consequently, PET with intact antibodies is unlikely to develop into a generally used diagnostic modality.

To optimize imaging characteristics of these radiopharmaceuticals focus is shifting towards smaller antibody-fragments (i.e., affibodies, diabodies, nanobodies, etc) and small molecules. These compounds have faster kinetics, thus radiolabeling with alternative positron emitters like ^{68}Ga, ^{18}F and ^{64}Cu becomes possible. The shorter residence time in the body and physical half-life of these isotopes results in a lower radiation dose to the patient. A good example of this approach is the recently published studies with ^{18}F-labelled and ^{68}Ga-labelled PSMA-targeting small molecules. Cho et al. showed the feasibility of ^{18}F-DCFBC PET only 2 hours after injection in five men with proven prostate carcinoma [64]. Afshar-Oromieh et al. successfully demonstrated PET with a ^{68}Ga-HBEDCC-PSMA molecule in 37 men only 1 and 3 hours after injection [65]. Though both radiopharmaceuticals are small molecules that target the PSMA-receptor, their distribution pattern on PET is quite different. Illustrating that the pharmacokinetic and targeting properties of antibody-fragments can differ significantly among ligands. In drug development, agreement between the study-drug and radiopharmaceutical is crucial when performing biodistribution and targeting studies. However, when imaging is primarily used as a biomarker to select patients, characterize lesions or assess treatment response, absolute accordance in biodistribution between study-drug and radiopharmaceutical is lesscrucial [66].

The complete picture

The fact that cancer is an extremely complex molecular disease that is dependent on local tissue for oncogenesis and growth is conceptualized by Hanahan and Weinberg through their 'Hallmarks of cancer' [67]. The tumor microenvironment is defined as the surrounding of the cancer cells including seemingly 'normal' biological processes and cells that support tumor growth such as blood vessels, immune inflammatory cells, cancer-associated fibroblasts, endothelial cells, extracellular matrix and signaling molecules. As briefly mentioned before, standard tumor stratification or evaluation of response generally do not recon with the microenvironment. Standard biopsies and the *ex vivo* assessments such as histology, proteomics, genomics, etc. only focus on a small area of the tumor at one specific moment in time. Still, even in a biopsy sample heterogeneity can already be appreciated through the varying degrees of cell proliferation, invasiveness, inflammation, receptor expression, vascularity, etc.

Molecular imaging can provide a more complete systematic picture of all these aspects in the living tumor, as is stated by Weissleder and Mahmood [68]. Well-known technologies that enable *in vivo* imaging of tumor physiology and the microenvironment include multi-parametric MRI, nuclear and optical imaging (e.g., relies on fluorescence, bioluminescence, reflectance or absorbance of light). Specialized algorithms are then applied to extract quantitative measures for signal intensity, shape and texture of the cancerous tissues, a novel methodology known as 'Radiomics'. This approach of transferring imaging data into phenotypic tumor information has been shown by Aerts et al. in over 1000 patients with lung and head/neck cancer [69]. With this broad range of technologies, even the term 'virtual molecular imaging biopsy' has been suggested to study the cancerous tissues as an alternative to standard biopsies [68]. Although medical imaging has indeed gained a central role in personalized medicine, standard biopsies still remain a crucial part of tumor identification. Combining the image-based phenotypic information with data gathered from *ex vivo* assessments of specific areas results in a synergistic approach to identity the heterogeneous tumor and measure response to targeted therapies.

CONCLUDING REMARKS

Advances in oncological sciences led to the development of novel anticancer agents that are designed to affect key molecular pathways or drivers. Nuclear molecular imaging techniques hold

great potential in clinical trials for selecting patients, characterize tumor lesions, assess pharmacokinetics and biodistribution, confirm drug targeting and optimize treatment schemes. In this respect, sensitive, reproducible and quantifiable whole body *in vivo* imaging techniques like PET are required. Though, this paper has provided a brief overview, the experience with immuno-radiopharmaceuticals in humans is building, and new labeled antibody (-derivates) are still being introduced in the clinical setting.

REFERENCES

1. Chabner BA, Roberts TG Jr. Timeline: Chemotherapy and the war on cancer. Nat Rev Cancer. 2005; 5: 65-72.
2. Yap TA, Sandhu SK, Workman P, de Bono JS. Envisioning the future of early anticancer drug development. Nat Rev Cancer. 2010; 10: 54-523.
3. Marchetti S, Schellens JH. The impact of FDA and EMEA guidelines on drug development in relation to Phase 0 trials. Br J Cancer. 2007; 97: 577-58.
4. Tan DS, Thomas GV, Garrett MD, Banerji U, de Bono JS, Kaye SB, Workman P. Biomarker-driven early clinical trials in oncology: a paradigm shift in drug development. Cancer J. 2009; 5: 406-420.
5. Smith JJ, Sorensen AG, Thrall JH. Biomarkers in imaging: realizing radiology's future. Radiology. 2003; 227: 633-638.
6. Bergström M, Grahnén A, Långström B. Positron emission tomography microdosing: a new concept with application in tracer and early clinical drug development. Eur J Clin Pharmacol. 2003; 59: 357-366.
7. Lappin G, Garner DRC. A Review of Human Phase 0 (Micro dosing) Clinical Trials Following the US Food and Drug Administration Exploratory Investigational New Drug Studies Guidance. Int J Pharm Med. 2006; 20: 59–65.
8. Marathe PH, Shyu WC, Humphreys WG. The use of radiolabeled compounds for ADME studies in discovery and exploratory development. Curr Pharm Des. 2004; 10: 2991-3008.
9. Isin EM, Elmore CS, Nilsson GN, Thompson RA, Weidolf L. Use of radiolabeled compounds in drug metabolism and pharmacokinetic studies. Chem Res Toxicol. 2012; 25: 532-542.
10. Weber J, Haberkorn U, Mier W. Cancer Stratification by Molecular Imaging. Int J Mol Sci. 20l5; 16: 4918–4946.
11. Uh P, Fricker G, Haberkorn U, Mier W. Radionuclides in drug development. Drug Discov Today. 2015; 20: 98-208.
12. Solon EG, Schweitzer A, Stoeckli M, Prideaux B. Autoradiography, MALDI-MS, and SIMS-MS imaging in pharmaceutical discovery and development. AAPS J. 2010; 12: -26.
13. Lietz CB, Gemperline E, Li L. Qualitative and quantitative mass spectrometry imaging of drugs and metabolites. Adv Drug Deliv Rev. 2013; 65: 074-085.
14. Solon EG. Autoradiography: high-resolution molecular imaging in pharmaceutical discovery and development. Expert Opin Drug Discov. 2007; 2: 503-54.
15. Solon EG. Autoradiography techniques and quantification of drug distribution. Cell Tissue Res. 2015; 360: 87-07.
16. Rahmim A, Zaidi H. PET versus SPECT: strengths, limitations and challenges. Nucl Med Commun. 2008; 29: 93-207.
17. Chen K, Chen X. Positron emission tomography imaging of cancer biology: current status and future prospects. Semin Oncol. 2011; 38: 70-86.
18. Judenhofer MS, Wehrl HF, Newport DF, Catana C, Siegel SB, Becker M, Thielscher A. Simultaneous PET-MRI: a new approach for functional and morphological imaging. Nat Med. 2008; 4: 459-465.
19. van der Have F, Vastenhouw B, Ramakers RM, Branderhorst W, Krah JO, Ji C, Staelens SG. U-SPECT-II: An Ultra-High-Resolution Device for Molecular Small-Animal Imaging. J Nucl Med. 2009; 50: 599-605.
20. Davies AJ. Radioimmunotherapy for B-cell lymphoma: Y90 ibritumomab tiuxetan and I(3) tositumomab. Oncogene. 2007; 26: 364-3628.
21. Perk LR, Visser OJ, Stigter-van Walsum M, Vosjan MJ, Visser GW, Zijlstra JM, Huijgens PC. Preparation and evaluation of (89)Zr-Zevalin for monitoring of (90)Y-Zevalin biodistribution with positron emission tomography. Eur J Nucl Med Mol Imaging. 2006; 33: 337-345.
22. Natarajan A, Gambhir SS. Radiation Dosimetry Study of [(89)Zr] rituximab Tracer for Clinical Translation of B cell NHL Imaging using Positron Emission Tomography. Mol Imaging Biol. 2014; 1-9.
23. Natarajan A, Arksey N, Iagaru A, Chin FT, Gambhir SS. Validation of 64Cu-DOTA-rituximab injection preparation under good manufacturing practices: a PET tracer for imaging of B-cell non-Hodgkin lymphoma. Mol Imaging. 2015; 4.
24. Sjögreen-Gleisner K, Dewaraja YK, Chiesa C, Tennvall J, Lindén O, Strand SE, Ljungberg M. Dosimetry in patients with B-cell lymphoma treated with [(90)Y]ibritumomab tiuxetan or [(3)I]tositumomab. Q J Nucl Med Mol Imaging. 2011; 55: 126-154.
25. Leahy MF, Seymour JF, Hicks RJ, Turner JH. Multicenter phase II clinical study of iodine-3-rituximab radioimmunotherapy in relapsed or refractory indolent non-Hodgkin's lymphoma. J Clin Oncol. 2006; 24: 4418-4425.
26. Rizvi SN, Visser OJ, Vosjan MJ, van Lingen A, Hoekstra OS, Zijlstra JM, Huijgens PC. Biodistribution, radiation dosimetry and scouting of 90Y-ibritumomab tiuxetan therapy in patients with relapsed B-cell non-Hodgkin's lymphoma using 89Zr-ibritumomab tiuxetan and PET. Eur J Nucl Med Mol Imaging. 2012; 39: 512-520.
27. Börjesson PK, Jauw YW, Boellaard R, de Bree R, Comans EF, Roos JC, Castelijns JA. Performance of immuno-positron emission tomography with zirconium-89-labeled chimeric monoclonal antibody U36 in the detection of lymph node metastases in head and neck cancer patients. Clin Cancer Res. 2006; 2: 233-240.
28. Börjesson PK, Jauw YW, de Bree R, Roos JC, Castelijns JA, Leemans CR, van Dongen GA. Radiation dosimetry of 89Zr-labeled chimeric monoclonal antibody U36 as used for immuno-PET in head and neck cancer patients. J Nucl Med. 2009; 50:1828-1836.
29. Vugts DJ, Heuveling DA, Stigter-van Walsum M, Weigand S, Bergstrom M, van Dongen GA, Nayak TK. Preclinical evaluation of 89Zr-labeled anti-CD44 monoclonal antibody RG7356 in mice and cynomolgus monkeys: Prelude to Phase clinical studies. MAbs. 2013; 6: 567-575.
30. Perik PJ, Lub-de Hooge MN, Gietema JA, van der Graaf WTA, de Korte MA, Jonkman S, et al. Indium-11-labeled trastuzumab scintigraphy in patients with human epidermal growth factor receptor 2-positive metastatic breast cancer. J Clin Oncol. 2006; 24: 2276–2282.
31. Dijkers EC, Kosterink JG, Rademaker AP, Perk LR, van Dongen GA, Bart J, de Jong JR. Development and characterization of clinical-grade 89Zr-trastuzumab for HER2/neu immunoPET imaging. J Nucl Med. 2009; 50: 974-981.
32. Dijkers EC, Oude Munnink TH, Kosterink JG, Brouwers AH, Jager PL, de Jong JR, van Dongen GA. Biodistribution of 89Zr-trastuzumab and PET imaging of HER2-positive lesions in patients with metastatic breast cancer. Clin Pharmacol Ther. 2010; 87: 586-592.
33. Mortimer JE, Bading JR, Colcher DM, Conti PS, Frankel PH, Carroll

MI, Tong S. Functional imaging of human epidermal growth factor receptor 2-positive metastatic breast cancer using (64)Cu-DOTA-trastuzumab PET. J Nucl Med. 2041; 55: 23-29.

34. Tamura K, Kurihara H, Yonemori K, Tsuda H, Suzuki J, Kono Y, Honda N. 64Cu-DOTA-trastuzumab PET imaging in patients with HER2-positive breast cancer. J Nucl Med. 2013; 54: 869-875.

35. Holland JP, Caldas-Lopes E, Divilov V, Longo VA, Taldone T, Zatorska D, Chiosis G. Measuring the pharmacodynamic effects of a novel Hsp90 inhibitor on HER2/neu expression in mice using Zr-DFO-trastuzumab. PLoS One. 2010; 5: 8859.

36. Janjigian YY, Viola-Villegas N, Holland JP, Divilov V, Carlin SD, Gomes-DaGama EM, Chiosis G. Monitoring afatinib treatment in HER2-positive gastric cancer with 8F-FDG and 89Zr-trastuzumab PET. J Nucl Med. 2013; 54: 936-943.

37. Gaykema SB, Schröder CP, Vitfell-Rasmussen J, Chua S, Oude Munnink TH, Brouwers AH, Bongaerts AH. 89Zr-trastuzumab and 89Zr-bevacizumab PET to evaluate the effect of the HSP90 inhibitor NVP-AUY922 in metastatic breast cancer patients. Clin Cancer Res. 2014; 20: 3945-3954.

38. Gebhart G, Lamberts LE, Garcia C. PET/CT with 89Zr-trastuzumab and 18F-FDG to individualize treatment with trastuzumab emtansine (T-DM) in metastatic HER2 positive breast cancer. J Clin Oncol. 2014.

39. Gaykema SB, Brouwers AH, Hovenga S, Lub-de Hooge MN, de Vries EG, Schröder CP,. Zirconium-89-trastuzumab positron emission tomography as a tool to solve a clinical dilemma in a patient with breast cancer. J Clin Oncol. 2012; 30: 74-75.

40. Cai W, Chen K, Mohamedali KA, Cao Q, Gambhir SS, Rosenblum MG, Chen X. PET of vascular endothelial growth factor receptor expression. J Nucl Med. 2006; 47: 2048-2056.

41. van der Bilt AR, Terwisscha van Scheltinga AG, Timmer-Bosscha H, Schröder CP, Pot L, Kosterink JG, van der Zee AG. Measurement of tumor VEGF-A levels with 89Zr-bevacizumab PET as an early biomarker for the antiangiogenic effect of everolimus treatment in an ovarian cancer xenograft model. Clin Cancer Res. 2012; 18: 6306-6314.

42. van Asselt SJ, Oosting SF, Brouwers AH, Bongaerts AH, de Jong JR, Lub-de Hooge MN, Oude Munnink TH. Everolimus Reduces (89) Zr-Bevacizumab Tumor Uptake in Patients with Neuroendocrine Tumors. J Nucl Med. 2014; 55: 1087-1092.

43. Oosting SF, Brouwers AH, van Es SC, Nagengast WB, Oude Munnink TH, Lub-de Hooge MN, Hollema H. 89Zr-bevacizumab PET visualizes heterogeneous tracer accumulation in tumor lesions of renal cell carcinoma patients and differential effects of antiangiogenic treatment. J Nucl Med. 2015; 56: 63-69.

44. Bergmann L, Kube U, Doehn C, Steiner T, Goebell PJ, Kindler M, et al. Everolimus in metastatic renal cell carcinoma after failure of initial anti–VEGF therapy: final results of a noninterventional study. BMC Cancer. 2015; 15: 303.

45. Gaykema SB, Brouwers AH, Lub-de Hooge MN, Pleijhuis RG, Timmer-Bosscha H, Pot L, van Dam GM. 89Zr-bevacizumab PET imaging in primary breast cancer. J Nucl Med. 2013; 54: 1014-1018.

46. Ping Li W, Meyer LA, Capretto DA, Sherman CD, Anderson CJ. Receptor-binding, biodistribution, and metabolism studies of 64Cu-DOTA-cetuximab, a PET-imaging agent for epidermal growth-factor receptor-positive tumors. Cancer Biother Radiopharm. 2008; 23: 158-171.

47. Aerts HJ, Dubois L, Hackeng TM, Straathof R, Chiu RK, Lieuwes NG, Jutten B. Development and evaluation of a cetuximab-based imaging probe to target EGFR and EGFRvIII. Radiother Oncol. 2007; 83: 326-332.

48. Cai W, Chen K, He L, Cao Q, Koong A, Chen X,. Quantitative PET of EGFR expression in xenograft-bearing mice using 64Cu-labeled cetuximab, a chimeric anti-EGFR monoclonal antibody. Eur J Nucl Med Mol Imaging. 2007; 34: 850-858.

49. Niu G, Sun X, Cao Q, Courter D, Koong A, Le QT, Gambhir SS. Cetuximab-based immunotherapy and radioimmunotherapy of head and neck squamous cell carcinoma. Clin Cancer Res. 2010; 6: 2095-2105.

50. Niu G, Li Z, Xie J, Le QT, Chen X. PET of EGFR antibody distribution in head and neck squamous cell carcinoma models. J Nucl Med. 2009; 50: 1116-1123.

51. Chang AJ, De Silva RA, Lapi SE. Development and characterization of 89Zr-labeled panitumumab for immuno-positron emission tomographic imaging of the epidermal growth factor receptor. Mol Imaging. 2013; 12: 17-27.

52. Aerts HJ, Dubois L, Perk L, Vermaelen P, van Dongen GA, Wouters BG, Lambin P. Disparity between in vivo EGFR expression and 89Zr-labeled cetuximab uptake assessed with PET. J Nucl Med. 2009; 50: 123-131.

53. Makris NE, Boellaard R, van Lingen A, Lammertsma AA, van Dongen GA, Verheul HM, Menke CW. PET/CT-derived whole-body and bone marrow dosimetry of 89Zr-cetuximab. J Nucl Med. 2015; 56: 249-254.

54. Taneja SS. ProstaScint(R) Scan: Contemporary Use in Clinical Practice. Rev Urol. 2004; 6: 19-28.

55. Holland JP, Divilov V, Bander NH, Smith-Jones PM, Larson SM, Lewis JS. 89Zr-DFO-J59 for immunoPET of prostate-specific membrane antigen expression in vivo. J Nucl Med. 2010; 5: 1293-1300.

56. Osborne JR, Green DA, Spratt DE, Lyashchenko S, Fareedy SB, Robinson BD, et al. A prospective pilot study of (89)Zr-J59/prostate specific membrane antigen positron emission tomography in men with localized prostate cancer undergoing radical prostatectomy. J Urol. 2014; 191: 1439–1445.

57. Osborne JR, Akhtar NH, Vallabhajosula S, Anand A, Deh K, Tagawa ST. Prostate-specific membrane antigen-based imaging. Urol Oncol. 2013; 31: 144-154.

58. Vargas HA, Grimm J, F Donati O, Sala E, Hricak H. Molecular imaging of prostate cancer: translating molecular biology approaches into the clinical realm. Eur Radiol. 2015; 25: 1294-1302.

59. Oosterwijk-Wakka JC, Boerman OC, Mulders PFA, Oosterwijk E. Application of Monoclonal Antibody G250 Recognizing Carbonic Anhydrase IX in Renal Cell Carcinoma. International Journal of Molecular Sciences. 2013; 14: 11402–11423.

60. Divgi CR, Pandit-Taskar N, Jungbluth AA, Reuter VE, Gönen M, Ruan S, et al. Preoperative characterization of clear-cell renal carcinoma using iodine-24-labelled antibody chimeric G250 (24I-cG250) and PET in patients with renal masses: a phase I trial. Lancet Oncol. 2007; 8: 304–310.

61. Pryma DA, O'Donoghue JA, Humm JL, Jungbluth AA, Old LJ, Larson SM, Divgi CR. Correlation of in vivo and in vitro measures of carbonic anhydrase IX antigen expression in renal masses using antibody 24I-cG250. J Nucl Med. 2011; 52: 535-540.

62. Divgi CR, Uzzo RG, Gatsonis C, Bartz R, Treutner S, Yu JQ, Chen D. Positron emission tomography/computed tomography identification of clear cell renal cell carcinoma: results from the REDECT trial. J Clin Oncol. 203; 3: 87-94.

63. Cheal SM, Punzalan B, Doran MG, Evans MJ, Osborne JR, Lewis JS, et al. Pairwise comparison of 89Zr- and 24I-labeled cG250 based on positron emission tomography imaging and nonlinear immunokinetic

modeling: in vivo carbonic anhydrase IX receptor binding and internalization in mouse xenografts of clear-cell renal cell carcinoma. Eur J Nucl Med Mol Imaging. 2014; 41: 985–994.

64. Cho SY, Gage KL, Mease RC, Senthamizhchelvan S, Holt DP, Jeffrey-Kwanisai A, et al. Biodistribution, tumor detection, and radiation dosimetry of 8F-DCFBC, a low-molecular-weight inhibitor of prostate-specific membrane antigen, in patients with metastatic prostate cancer. J Nucl Med. 2012; 53: 1883–1891.

65. Afshar-Oromieh A, Malcher A, Eder M, Eisenhut M, Linhart HG, Hadaschik BA, et al. PET imaging with a [68Ga]gallium-labelled PSMA ligand for the diagnosis of prostate cancer: biodistribution in humans and first evaluation of tumour lesions. Eur J Nucl Med Mol Imaging. 2013; 40: 486–495.

66. Heukelom J, Hamming O, Bartelink H, Hoebers F, Giralt J, Herlestam T, Verheij M. Adaptive and innovative Radiation Treatment FOR improving Cancer treatment outcomE (ARTFORCE); a randomized controlled phase II trial for individualized treatment of head and neck cancer. BMC Cancer. 2013; 13: 84.

67. Hanahan D, Weinberg RA. Hallmarks of cancer: the next generation. Cell. 2011; 144: 646-674.

68. Weissleder R, Mahmood U. Molecular imaging. Radiology. 2001; 219: 316-333.

69. Aerts HJ, Velazquez ER, Leijenaar RT, Parmar C, Grossmann P, Carvalho S, Bussink J. Decoding tumour phenotype by noninvasive imaging using a quantitative radiomics approach. Nat Commun. 2014; 5: 4006.

Cite this article

van der Veen BJW, Stokkel MPM (2015) The clinical role of nuclear imaging in immunotherapeutic drug development. J Pharmacol Clin Toxicol 3(4):1057.